

# Thermal diffusivity of reaction-sintered $\text{AlON}/\text{Al}_2\text{O}_3$ particulate composites

Y.W. Kim<sup>a</sup>, Y.W. Oh<sup>b</sup>, S.Y. Yoon<sup>c</sup>, R. Stevens<sup>d</sup>, H.C. Park<sup>c,\*</sup>

<sup>a</sup>Functional Materials Research Team, Research Institute of Industrial Science and Technology, Pohang 790-330, South Korea

<sup>b</sup>Department of Materials Science and Engineering, Kyungnam University, Masan 631-701, South Korea

<sup>c</sup>School of Materials Science and Engineering, Pusan National University, Pusan 609-735, South Korea

<sup>d</sup>Department of Engineering and Applied Science, University of Bath, Bath BA2 7AY, UK

Received 19 April 2007; received in revised form 14 May 2007; accepted 22 June 2007

Available online 10 August 2007

## Abstract

The thermal diffusivity of particulate composites prepared by sintering compacts of  $\text{Al}_2\text{O}_3$  with additions of 1–25 mol%  $\text{AlN}$  under 1-atm nitrogen gas pressure at 1600–1800 °C has been measured over the range 25–1000 °C using the laser flash method. The diffusivity of reaction-sintered materials decreased on addition of  $\text{AlN}$ , mainly due to the formation of an  $\text{AlON}$  phase. This effect was less pronounced with increasing temperature and furthermore, it appeared to be related to the temperature-dependence of thermal resistance. The influence of crystalline phase, microstructure and physical property on the thermal diffusivity of  $\text{AlON}/\text{Al}_2\text{O}_3$  was characterized. The thermal conductivity of the sintered materials at room temperature behaved in a similar manner to the thermal diffusivity.

© 2007 Elsevier Ltd and Techna Group S.r.l. All rights reserved.

**Keywords:** A. Sintering; B. Composites; C. Thermal properties; E. Structural applications

## 1. Introduction

Dense polycrystalline aluminum oxynitride spinel ( $\text{AlON}$ ) and aluminum oxide ( $\text{Al}_2\text{O}_3$ ) are useful structural and optical ceramics [1]. However, unlike  $\text{Al}_2\text{O}_3$ , which due to its crystal form is anisotropic,  $\text{AlON}$  is an isotropic material, this allowing fabrication of optically transparent polycrystalline material [2]. Corbin [3] has reviewed the processing, structure and mechanical properties of  $\text{AlON}$ .

The phase stability of  $\text{Al}_2\text{O}_3$  is well established and documented. However, there are disagreements about the extent of the stability region of  $\text{AlON}$  in the  $\text{Al}_2\text{O}_3$ – $\text{AlN}$  system. This is believed to be due to  $\text{AlON}$  being found only under a limited range of oxygen and nitrogen pressures and the formation of  $\text{AlON}$  being too slow to reach equilibrium at temperatures less than 1750 °C [4].  $\text{AlON}$  itself has a stoichiometric composition  $5\text{AlN} \cdot 9\text{Al}_2\text{O}_3$  and melts incongruently into an alumina-rich, stable liquid and a second nitride-rich unstable (volatile) liquid, at approximately 2050 °C [2].

From a practical point of view, the evaluation of important properties such as thermal-shock resistance is often required for high-temperature structural materials and this involves determination of heat flow and heat flow rates. Two fundamental properties needed for evaluation of materials are thus the thermal diffusivity ( $\alpha$ ) and thermal conductivity ( $k$ ); the relationship between these properties can be expressed simply as follow:

$$\alpha = \frac{k}{\rho c_p}, \quad (1)$$

where  $c_p$  is the specific heat at constant pressure and  $\rho$  is bulk density. Thermal conductivity can be determined from the straightforward measurements of thermal diffusivity, specific heat and bulk density.

For thermal shock applications and heat flow calculations, the conductivity is important primarily in steady-state conditions, whereas the diffusivity is of interest in transient heat flow situations. Also, thermal diffusivity has significance when discussing the phonon scattering process since the mean free path of the scattered phonons is more directly related to the diffusivity than to conductivity. Several authors have reported

\* Corresponding author. Tel.: +82 51 510 2392; fax: +82 51 512 0528.

E-mail address: [hcpark1@pusan.ac.kr](mailto:hcpark1@pusan.ac.kr) (H.C. Park).

on the thermal diffusivity in the  $\text{Al}_2\text{O}_3$ –AlN system. The thermal diffusivity at 300 and 450 K of the AlON containing 39.1 mol% oxygen was measured by Sakai et al. [5], who reported values of 0.043 and 0.027  $\text{cm}^2/\text{s}$ , respectively. Quinn et al. [6] reported similar results on AlON prepared by reaction sintering  $\text{Al}_2\text{O}_3$  with additions of 30 mol% AlN (0.037  $\text{cm}^2/\text{s}$ ) and 35.7 (0.040  $\text{cm}^2/\text{s}$ ).

In previous studies, we investigated reaction sintering, phase stability, microstructure and mechanical properties in the system  $\text{Al}_2\text{O}_3$ –AlN [7,8]; the stability of the individual crystalline phase and microstructure were dependent on both sintering temperature and batch composition. The objective of this work has been to study the effect of crystalline phase and microstructure on the thermal diffusivity of materials sintered in the  $\text{Al}_2\text{O}_3$  system with 1–25 mol% AlN additions. Owing to the remaining presence of the more sinterable  $\text{Al}_2\text{O}_3$  in the composite system, an investigation of further dense structural materials by reaction sintering was undertaken.

## 2. Experimental procedure

$\text{Al}_2\text{O}_3$  (99.8% in purity, AES 11C, Sumitomo Chemicals) was intimately mixed with 1–25 mol% AlN (grade F, Tokuyama Soda). The AlN powder composition was analyzed as Ca 75 ppm, Mg 2 ppm, Cr < 10 ppm, Fe < 10 ppm, Si 36 ppm, Ni < 10 ppm, Al 65.4%, O 1.0%, C 0.06% and N 33.5%. The mean particle size and specific surface area of the  $\text{Al}_2\text{O}_3$  powder were 2.1  $\mu\text{m}$  and 4.1  $\text{m}^2/\text{g}$ , respectively, and those of the AlN powder were 0.4  $\mu\text{m}$  and 8.2  $\text{m}^2/\text{g}$ .

The batch powders were mixed and homogenized by ball milling in ethanol for 48 h using a high-density polyethylene bottle with alumina ball media; 0.3 wt% deflocculant (DARVAN-C, R.T. Vanderbilt) and 0.5 wt% binder (PVA, Aldrich) were used. After drying, the mixed powders were deagglomerated in an agate mortar and passed through a 50 mesh nylon sieve.

Cylindrical compacts (10 mm diameter  $\times$  5 mm thick) were prepared by die pressing under 70 MPa, followed by cold isostatic pressing under 200 MPa. The compacts were then calcined at 500  $^\circ\text{C}$  in air to remove organic residue. Subsequently, the samples were placed in a graphite crucible, embedded in aluminum nitride powder and then sintered in a graphite resistance furnace at temperature in the range 1600–1800  $^\circ\text{C}$  for 2 h, at 1 atm nitrogen pressure.

Crystalline phases were identified by XRD. The sintered density was determined directly by dividing the mass by the volume of samples. The surface microstructures of the sintered materials were observed using a scanning electron microscope (SEM, MK3, Cambridge) after polishing with 1  $\mu\text{m}$  diamond slurry and thermal etching at 1400  $^\circ\text{C}$  for 30 min. The nitrogen content in the sintered specimens was determined using a nitrogen/oxygen determinator (TC-230, Leco).

The thermal diffusivity was measured by means of the laser flash technique [9], using a ruby laser ( $\lambda = 0.6943 \mu\text{m}$ ) and an InSb infrared detector (TC-7000, Shinku-Riko Co.), at temperatures in the range 25–1000  $^\circ\text{C}$ . Specimens were in the form of discs, 8.5 mm in diameter and 1.8–3.8 mm in thickness. Both sides were polished and then coated with a sputtered gold film to prevent direct transmission of the laser beam. They were subsequently treated to deposit a colloidal carbon film to increase the absorption of the laser beam.

## 3. Results and discussion

The crystalline phase, bulk density and nitrogen content in the sintered materials [8] are summarized in Table 1. After sintering at 1600  $^\circ\text{C}$ , all specimens consisted of  $\alpha$ - $\text{Al}_2\text{O}_3$  and AlON phases, regardless of the quantity of AlN added. The amount of AlON present increased with increasing AlN addition. The major phase of the specimen prepared with 25 mol% AlN was AlON. On sintering at 1700  $^\circ\text{C}$ , nearly all  $\text{Al}_2\text{O}_3$  in the specimens with  $\geq 20$  mol% AlN additions reacted

Table 1  
Crystalline phase, bulk density and nitrogen content of sintered materials

Sintering temperature ( $^\circ\text{C}$ )	AlN addition (mol%)	XRD peak intensity of crystalline phase <sup>a</sup>			Bulk density ( $\text{g}/\text{cm}^3$ )	Measured $\text{N}_2$ content (wt%)
		$\text{Al}_2\text{O}_3$	AlON	$5\text{Al}_2\text{O}_3 \cdot \text{AlN}$		
1600	1	h	tr	ND	3.54	0.11
	5	h	w	ND	3.23	0.77
	10	h	m	ND	2.99	1.11
	20	h	h	ND	2.76	1.76
	25	h	vh	ND	2.60	2.75
1700	1	h	tr	ND	3.85	0.22
	5	h	w	ND	3.67	1.10
	10	h	m	ND	3.38	1.87
	20	ND	h	ND	2.97	3.41
	25	ND	vh	ND	2.99	4.84
1800	1	h	tr	ND	3.89	0.11
	5	h	w	tr	3.77	0.77
	10	>m	m	m	3.54	1.54
	20	ND	h	ND	3.46	3.08
	25	ND	vh	ND	3.46	4.95

<sup>a</sup> Symbol legend for relative peak intensities: (vh) very high; (h) high; (m) middle; (w) weak; (tr) trace; (ND) not detected; (>m) somewhat higher than “m”.

to form AlON. The specimen with 5 mol% AlN addition sintered at 1800 °C consisted mainly of  $\alpha$ -Al<sub>2</sub>O<sub>3</sub> and minor amounts of AlON and  $\phi$  phase (5Al<sub>2</sub>O<sub>3</sub>·AlN, monoclinic). In the case of 10 mol% AlN addition, a significant amount of primary Al<sub>2</sub>O<sub>3</sub> had reacted and converted to AlON, and in the specimens with the additions of 20 and 25 mol% AlN, only AlON was present.

As expected, the sintered bulk density ( $\sim 94.5\%$  of theoretical density at 1800 °C with  $\geq 20$  mol% AlN additions) of the composites decreased with increasing AlN addition and increased with increasing sintering temperature.

Microstructures of polished and thermally etched surfaces of materials obtained by sintering at 1600–1800 °C for 2 h with additions of 1–25 mol% AlN are shown in Figs. 1–3. After sintering at 1600 °C (Fig. 1), the microstructure of the specimen with 1 mol% AlN addition was similar to that of sintered pure alumina. With increasing AlN addition, from 5 to 25 mol%, the amount of AlON and porosity present increased and at the same time, the grain growth of Al<sub>2</sub>O<sub>3</sub> appeared to have been suppressed. Overall, there was poor densification of the compact on sintering. In the specimens with 5 and 10 mol% AlN, it was possible to distinguish the Al<sub>2</sub>O<sub>3</sub> from AlON grains. However, in the specimen with 20 and 25 mol% AlN, this was no longer possible because the reaction of Al<sub>2</sub>O<sub>3</sub> and AlN had proceeded almost to completion.

On sintering at 1700 °C (Fig. 2), in the specimens with 5 and 10 mol% AlN additions, caused the AlON to be formed mainly at grain boundaries and at the triple points of the Al<sub>2</sub>O<sub>3</sub>, but in the case of additions of 25 mol% AlN, almost all the Al<sub>2</sub>O<sub>3</sub> was

converted into AlON. The reaction and sintering process occurred simultaneously to completion, but left significant amounts of isolated but large remnant pores uniformly distributed over wide areas of the sample (Fig. 2(d)). On sintering at 1800 °C, in the specimen with 5 mol% AlN, the alumina grains were homogeneous with a mean grain size of about 10.5  $\mu$ m and the formation of AlON tended to be located at the triple points (Fig. 3(b)). The morphology of the specimens with additions of 10 and 25 mol% AlN, sintered at 1800 °C (Fig. 3(c and d)) showed a further feature of interest. Even though undetected by XRD, a few remnant isolated alumina grains, which were surrounded by a fine AlON matrix, were present. A large quantity of liquid was formed at AlON grain boundaries, which had inhibited the grain growth of Al<sub>2</sub>O<sub>3</sub>. Grain growth was still observed but had necessarily taken place between adjacent Al<sub>2</sub>O<sub>3</sub> grains in the localized absence of AlN since dissolution of the Al<sub>2</sub>O<sub>3</sub> would have resulted in reaction with any AlN present. The grain growth of the matrix material in the specimen with 25 mol% AlN addition was more noticeable compared with the specimen having a 10 mol% AlN addition.

The thermal diffusivity values measured in the range 25–1000 °C for the specimens with additions of 1–25 mol% AlN, after sintering at 1600, 1700 and 1800 °C for 2 h under 1 atm nitrogen gas atmosphere are shown in Figs. 4–6. The temperature dependency of the thermal diffusivity of the specimens with additions of 1–10 mol% AlN was similar to that for the pure alumina [10]. This implies that the heat flow path is, as would be expected, principally through the continuous alumina phase

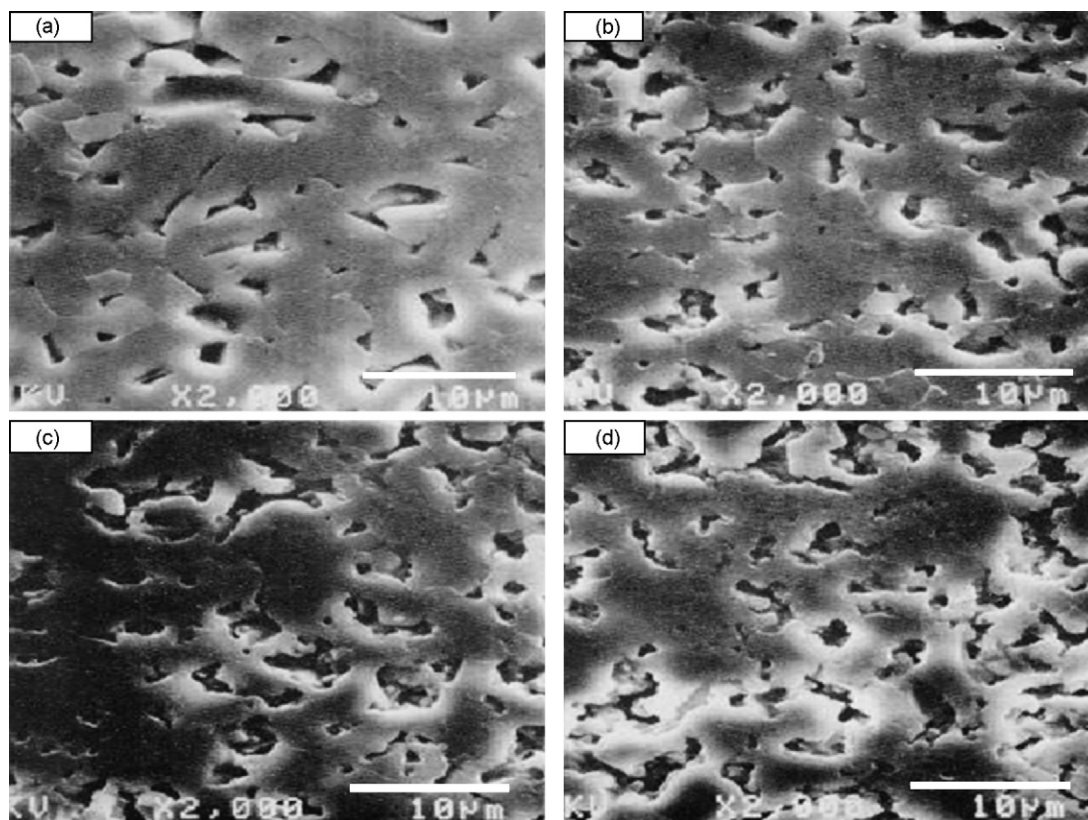


Fig. 1. Microstructures in the Al<sub>2</sub>O<sub>3</sub>–AlN system with additions of (a) 1, (b) 5, (c) 10 and (d) 20 mol% AlN, sintered at 1600 °C for 2 h.

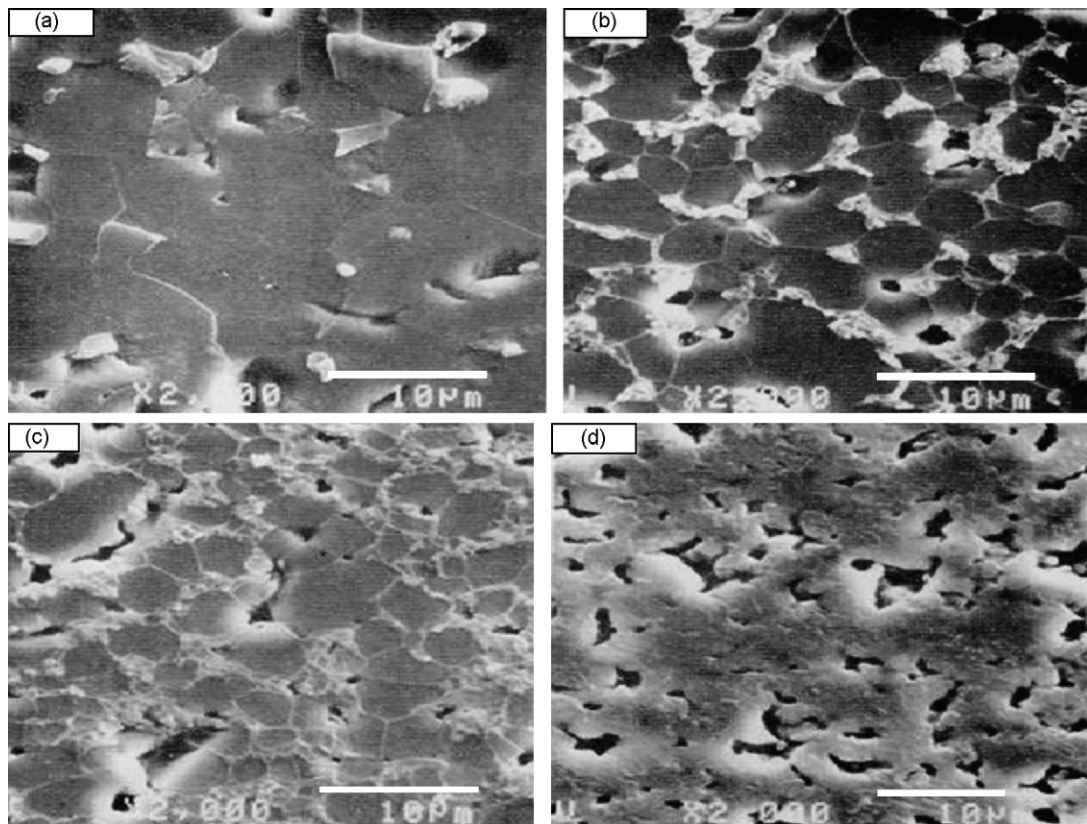


Fig. 2. Microstructures in the  $\text{Al}_2\text{O}_3$ -AlN system with additions of (a) 1, (b) 5, (c) 10 and (d) 20 mol% AlN, sintered at 1700 °C for 2 h.

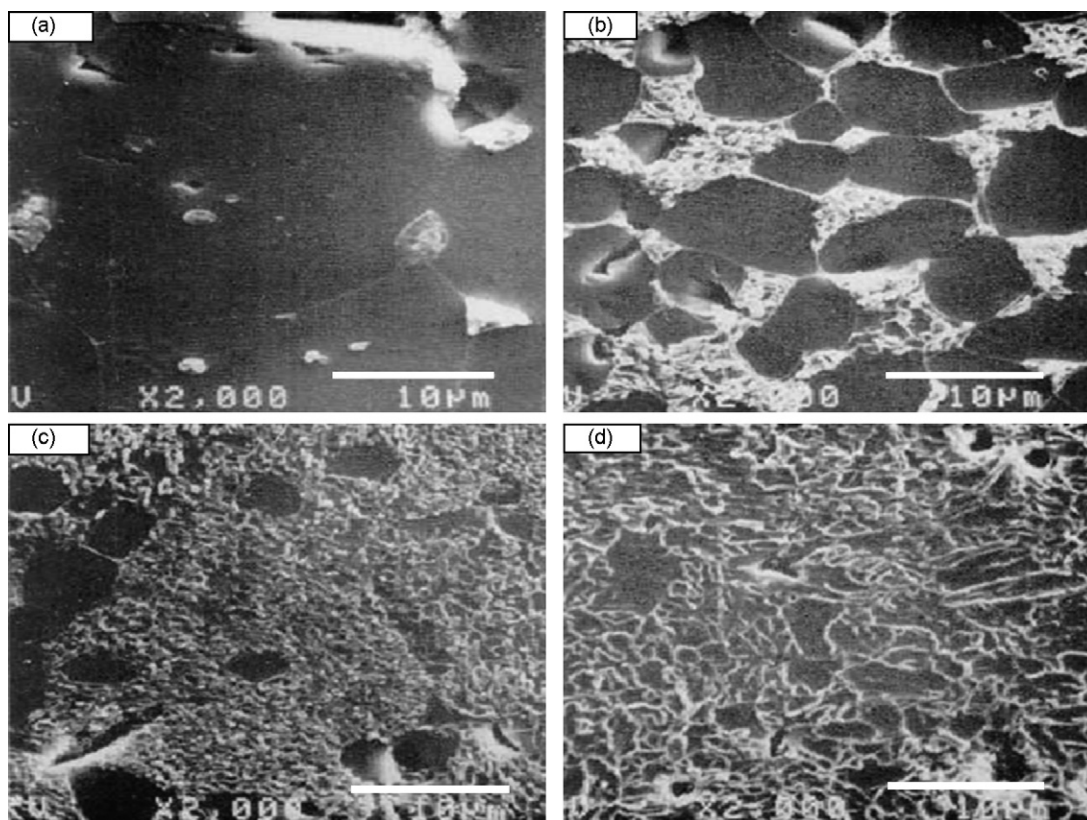


Fig. 3. Microstructures in the  $\text{Al}_2\text{O}_3$ -AlN system with additions of (a) 1, (b) 5, (c) 10 and (d) 25 mol% AlN, sintered at 1800 °C for 2 h.



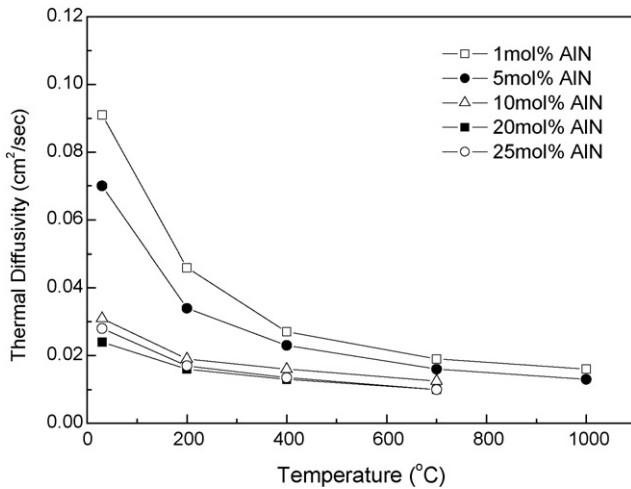


Fig. 4. Thermal diffusivity in the system  $\text{Al}_2\text{O}_3$ –AlN, sintered at 1600 °C for 2 h.

rather than the dispersed AlON. The mean free path of phonon movement decreases with increasing temperature,

$$\lambda \approx \frac{1}{T}, \quad (2)$$

since the more intense the thermal variations, the less regular the lattice structure becomes. Thus thermal diffusivity usually decreases as temperature is raised to higher levels. This trend coincided well with the results of this study. The thermal diffusivity of specimens obtained by sintering at 1600 °C with 1 mol% AlN addition, consisting mainly of  $\alpha$ - $\text{Al}_2\text{O}_3$  was similar to that reported by Plummer et al. at 25–1000 °C (0.093–0.014  $\text{cm}^2/\text{s}$ ) [10]. The thermal diffusivity values at 200 °C, of the specimens with 1 and 5 mol% AlN additions were reduced to about a half the values at 25 °C. For 10–25 mol% AlN additions, thermal diffusivity values at 25–300 °C were a half to a third compared to those with 1 and 5 mol% AlN addition. This lower thermal diffusivity in 10 mol% AlN addition compared with 5 mol% AlN could be due to a combination of the lower sintered density and to the

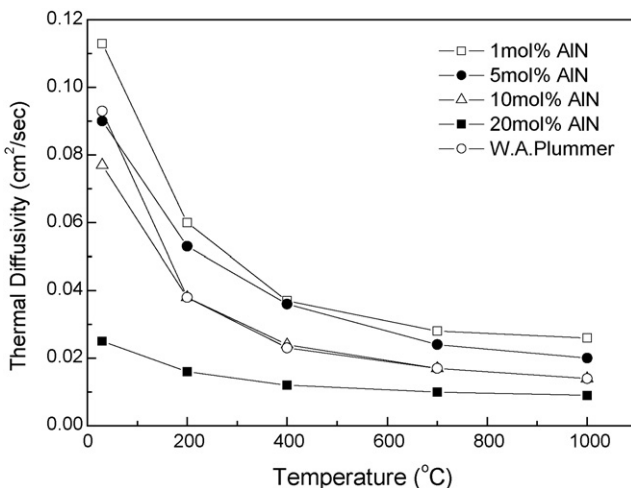


Fig. 5. Thermal diffusivity in the system  $\text{Al}_2\text{O}_3$ –AlN, sintered at 1700 °C for 2 h.

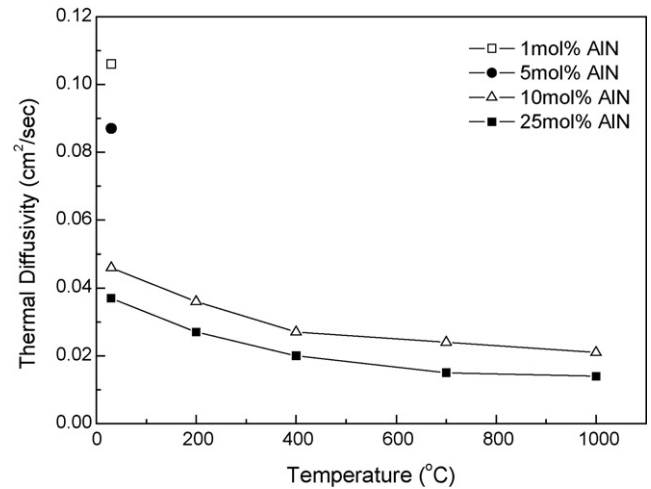


Fig. 6. Thermal diffusivity in the system  $\text{Al}_2\text{O}_3$ –AlN, sintered at 1800 °C for 2 h.

formation of relatively large amounts of AlON phase, which has a lower thermal diffusivity compared with  $\alpha$ - $\text{Al}_2\text{O}_3$ . After sintering at 1700 °C, the thermal diffusivity of the specimens with additions of 1–10 mol% AlN increased; for the 10 mol% AlN addition, especially, it was about twice as large as that of the specimen sintered at 1600 °C, due in this case to enhanced densification. The addition of 20 mol% AlN, however, did not give an increase in diffusivity due to the presence of the AlON matrix phase even though the specimen had an increased sintered density and hence a reduced porosity. This implies that the thermal diffusivity of the composite is more sensitive to continuous matrix phase rather than sintered density. The specimen with 20 mol% AlN consisted of a majority of AlON phase; its thermal diffusivity exhibited somewhat lower values than those reported by Sakai et al. [5] and by Quinn et al. [6], owing to differences in sintered density.

When one particulate phase is dispersed within a matrix of another phase, the bulk diffusivity can be handled mathematically by the following equation similar to that suggested by Kingery et al. [11]:

$$\lambda_B = \lambda_c \left[ \frac{1 + 2\lambda_d(1 - \lambda_c/\lambda_d)/(2\lambda_c/\lambda_d + 1)}{1 - \lambda_d(1 - \lambda_c/\lambda_d)/(2\lambda_c/\lambda_d + 1)} \right], \quad (3)$$

where the subscripts d and c refer to the dispersed and continuous phases. Eq. (3) is satisfactory at the compositional extremes, where the minor phase is truly dispersed, this corresponding to the compositions having additions of 1–10 mol% AlN in our experiments. In general, the bulk diffusivity of mixtures of phases exhibits intermediate values compared to those of each component phase; in such a case, however, the change in diffusivity does not always vary linearly with the phase quantities, because the heat flows through those microstructural paths of higher diffusivity and is restricted by the lower diffusivity phase. Using a micromechanics approach, it is possible to correlate continuum properties, such as diffusivity with microstructure and phase composition [12–14], but the difference generally obtained is small and can be related to the tortuosity of the thermal flux pathway.

The thermal diffusivity at  $> 25\text{ }^{\circ}\text{C}$  of specimens (8.5 mm diameter, 1.84 mm thick) with additions of 1 and 5 mol% AlN, sintered at  $1800\text{ }^{\circ}\text{C}$  could not be measured accurately because they exhibited a transmittance of about 26 and 34% at  $2000\text{ cm}^{-1}$ , respectively [15]. It is generally accepted that the laser flash method is not suitable for a sample with partial translucence or severe radiation loss [16]. The thermal diffusivity of specimens with additions of 1–10 mol% AlN, sintered at  $1800\text{ }^{\circ}\text{C}$  decreased somewhat compared with a specimen sintered at  $1700\text{ }^{\circ}\text{C}$ , due to the higher content of AlON phase formed. The thermal diffusivity for a 1 mol% AlN addition coincided relatively well with values for sintered alumina reported by Plummer et al. [10] and for Lucalox reported by Chang et al. [17], respectively, but on sintering at  $1700$  and  $1800\text{ }^{\circ}\text{C}$ , the thermal diffusivities were higher than their values. Generally, the relative effect of AlN addition on thermal diffusivity was reduced at the higher temperatures than at lower ones; a similar tendency had also been reported in the system  $\text{Al}_2\text{O}_3\text{--Cr}_2\text{O}_3$  [18] and  $\text{Al}_2\text{O}_3\text{--Ba-mica}$  [19].

Consideration of the relationship between thermal diffusivity and microstructure, for the specimens sintered at  $1800\text{ }^{\circ}\text{C}$  indicates that:

- the increase of  $\text{Al}_2\text{O}_3$  grain size had no significant effect on thermal diffusivity as long as the other factors (phase volume fraction, porosity) remained constant, in comparison with the specimens with 1 mol% AlN addition, sintered at  $1600$ ,  $1700$  and  $1800\text{ }^{\circ}\text{C}$ ;
- the presence of AlON as a second phase, notably at the triple points (Fig. 3(b)), having a lower thermal diffusivity than the matrix phase,  $\text{Al}_2\text{O}_3$ , decreased the diffusivity;
- the diffusivity was greatly lowered when the alumina grains became isolated by AlON (Fig. 3(c)), due to the heat flux becoming restricted by lower diffusivity phase, AlON;
- the glassy phase present in specimens with  $\geq 10$  mol% AlN additions caused a further reduction in diffusivity, presumably due to more interference for phonon movement, i.e., limiting the mean free path by the less ordered structure.

Thermal conductivity at room temperature of sintered materials with additions of 1–25 mol% AlN, as calculated using the Eq. (1) is shown in Fig. 7. As expected from Eq. (1), the thermal conductivity generally behaved in a similar manner to the thermal diffusivity, i.e., high thermal diffusivity gave high thermal conductivity. The thermal conductivity with 1 mol% AlN addition, sintered at  $1700\text{ }^{\circ}\text{C}$  was  $35.1\text{ W/mK}$ , similar to values measured using different methods by previous researchers [20,21]. After sintering at  $1800\text{ }^{\circ}\text{C}$ , the thermal conductivity in the specimens with additions of 20 and 25 mol% AlN was about  $10.4\text{ W/mK}$  similar to that obtained by Quinn et al. [6]; this higher thermal conductivity when compared with  $1600$  and  $1700\text{ }^{\circ}\text{C}$  sintered material is probably due to the improved densification of the AlON matrix, resulting in a decrease in porosity. Thermal conductivity,  $k$ , by transfer of phonons (lattice vibrations) may be determined from kinetic energy

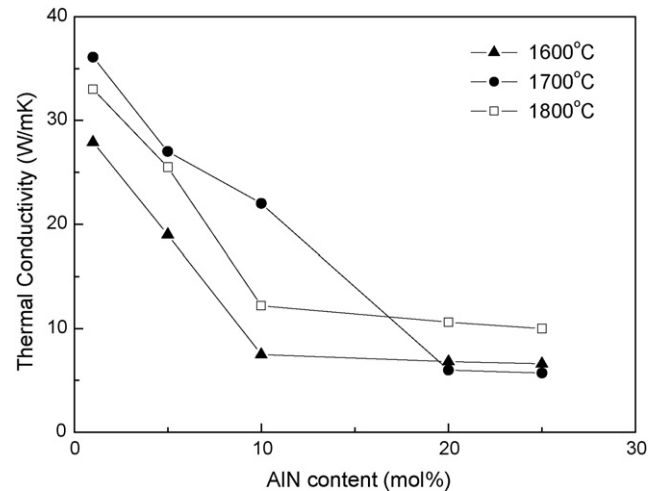


Fig. 7. Thermal conductivity in the system  $\text{Al}_2\text{O}_3\text{--AlN}$  as a function of AlN content added.

considerations as:

$$k = \frac{c_p v \lambda}{3} \quad (4)$$

in which  $c_p$  is the heat capacity,  $v$  the average velocity of a phonon and  $\lambda$  the mean free path of a phonon. At room temperature, any differences in the value of  $k$  are mainly governed by a change of  $\lambda$ , as affected by the combined influence of phonon–phonon collisions and phonon–lattice interactions, because values of  $c_p$  and  $v$  are relatively small. This indicates that the presence of a second phase, including pores, may have an influence on the thermal conductivity of ceramic composites. In spite of the higher quantity of AlON and glass phases present in the specimens with 20 and 25 mol% AlN additions, sintered at  $1800\text{ }^{\circ}\text{C}$ , compared with specimens sintered at  $1600$  and  $1700\text{ }^{\circ}\text{C}$ , their higher thermal conductivity is considered partially due to the decrease in porosity resulting on further densification.

#### 4. Conclusions

Two phase AlON– $\text{Al}_2\text{O}_3$  particulate composite materials can be prepared by the controlled atmosphere sintering at  $1600\text{--}1800\text{ }^{\circ}\text{C}$  of appropriate mixtures of fine particle size AlN and  $\text{Al}_2\text{O}_3$  powders. The thermal diffusivity of these materials was governed by three main microstructural features, dependent on the batch composition and sintering temperature, namely the nature of the major phase, the presence of a second phase (including pores) at grain boundaries and thirdly an intergranular glass. Of them, the presence of AlON particulate phase in the microstructure was most influential in reducing thermal diffusivity, compared with  $\text{Al}_2\text{O}_3$ -based materials. The effect of the amount of AlN added, on thermal diffusivity, appeared to be less on increasing the temperature in the range  $25\text{--}1000\text{ }^{\circ}\text{C}$ . The thermal diffusivity and thermal conductivity of sintered materials exhibited a similar tendency.

## Acknowledgements

This work was supported by grants-in-aid for the National Core Research Center Program from MOST/KOSEF (No. R15-2006-022-01001-0).

## References

- [1] J. Barata, J. Gorni, Improvements in mechanical and electrical properties of alumina, *Powder Metall. Int.* 4 (3) (1972) 124–128.
- [2] J.W. McCauley, N.D. Corbin, Phase relations and reaction sintering of transparent cubic aluminum oxynitride spinel (ALON), *J. Am. Ceram. Soc.* 62 (1979) 476–579.
- [3] N.D. Corbin, Aluminum oxynitride spinel: a review, *J. Eur. Ceram. Soc.* 5 (1989) 143–154.
- [4] H.X. Willems, M.M.R.M. Hendrix, G. de With, R. Metselaar, Thermodynamics of Alon II: phase relations, *J. Eur. Ceram. Soc.* 10 (1992) 339–346.
- [5] T. Sakai, M. Kuriyama, T. Inukai, T. Kizima, Effect of the oxygen impurity on the sintering and the thermal conductivity of AlN polycrystals, *Yokyo-Kyokai-Shi* 86 (4) (1978) 174–179.
- [6] C.D. Quinn, N.D. Corbin, J.W. McCauley, Thermochemical properties of aluminum oxynitride spinel, *Am. Ceram. Soc. Bull.* 63 (5) (1984) 723–730.
- [7] Y.W. Kim, B.H. Park, H.C. Park, Y.B. Lee, K.D. Oh, F.L. Riley, Sintering, microstructure and mechanical properties of AlIN-AlN particulate composites, *Br. Ceram. Trans.* 97 (1998) 97–104.
- [8] Y.W. Kim, H.C. Park, Y.B. Lee, K.D. Oh, R. Stevens, Reaction sintering and microstructural development in the system  $\text{Al}_2\text{O}_3$ –AlN, *J. Eur. Ceram. Soc.* 21 (2001) 2383–2391.
- [9] F. Righini, A. Cezairliyan, Pulse method of thermal diffusivity measurements (a review), *High Temp. High Press.* 5 (1973) 481–501.
- [10] W.A. Plummer, D.E. Campbell, A.A. Comstock, Method of measurement of thermal diffusivity to 1000 °C, *J. Am. Ceram. Soc.* 45 (7) (1962) 310–316.
- [11] W.D. Kingery, H.K. Bowen, D.R. Uhlmann, *Introduction to Ceramics*, John Wiley & Sons, USA, 1976.
- [12] J. Luo, R. Stevens, Micromechanics of randomly oriented ellipsoidal inclusion composites: part II, elastic moduli, *J. Appl. Phys.* 79 (1996) 9057–9063.
- [13] J. Luo, R. Taylor, R. Stevens, The physical properties of MgO/SiC composites, in: J.P. Singh, N.P. Bansal (Eds.), *Ceramic Transactions*, vol. 46, American Ceramic Society, Westerville, 1994, pp. 741–752.
- [14] J. Luo, R. Stevens, R. Taylor, Thermal diffusivity/conductivity of magnesium oxide/silicon carbide composites, *J. Am. Ceram. Soc.* 80 (3) (1997) 699–704.
- [15] Y.W. Kim, Ph.D. Thesis, Pusan National University, Pusan, South Korea, 1996.
- [16] R.L. Rudkin, R.J. Jenkins, W.J. Parker, Thermal diffusivity measurements on metals at high temperatures, *Rev. Sci. Instrum.* 33 (1962) 21–24.
- [17] H. Chang, M. Altman, R. Sharma, The determination of thermal diffusivities of thermal storage materials, part I: solids up to melting point, *J. Eng. Power* (1967) 407–414.
- [18] J.E. Matta, D.P.H. Hasselman, Thermal diffusivity of  $\text{Al}_2\text{O}_3$ – $\text{Cr}_2\text{O}_3$  solid solutions, *J. Am. Ceram. Soc.* 58 (9–10) (1975) 458.
- [19] G.E. Youngblood, L.D. Bentsen, J.W. McCauley, D.P.H. Hasselman, Thermal diffusivity of Ba-mica/alumina composites, *Am. Ceram. Soc. Bull.* 58 (6) (1979) 620–621.
- [20] M. McQuarrie, Thermal conductivity: VII, analysis of variation of conductivity with temperature for  $\text{Al}_2\text{O}_3$ , BeO and MgO, *J. Am. Ceram. Soc.* 37 (2) (1954) 91–95.
- [21] W. George, Thermal conductivity of alumina ceramics in the temperature range 40–400 °C, *Special Ceram.* 5 (1972) 211–223.